The ν_1 and ν_3 bands of $^{16}O_3$: Line positions and intensities

(16)03

J.-M. Flaud and C. Camy-Peyret
Laboratoire de Physique Moléculaire
et d'Optique Atmosphérique, CNRS,
Bât. 221, Campus d'Orsay, 91405 ORSAY CEDEX, France

V. Malathy Devi
Department of Physics
College of William and Mary
Williamsburg, Virginia 23185

C.P. Rinsland and M.A.H. Smith
Atmospheric Sciences Division
NASA Langley Research Center
Hampton, Virginia 23665

Manuscript pages: 14
Figures: 2
Tables: 5

Running title : ν_1 and ν_3 bands of $^{16}O_3$

Mail correspondence to :

Dr J.-M. Flaud
Laboratoire de Physique Moléculaire
et d'Optique Atmosphérique
Bât. 221, Campus d'Orsay
91405 ORSAY CEDEX, France

ABSTRACT

Using 0.005 cm^{-1}-resolution Fourier transform spectra of samples of ozone, the ν_1 and ν_3 bands of $^{16}O_3$ have been reanalyzed to obtain accurate line positions and an extended set of upper state rotational levels (J up to 69, K_a up to 20). Combined with the available microwave data, these upper state rotational levels were satisfactorily fitted using a Hamiltonian which takes explicitly into account the strong Coriolis interaction affecting the rotational levels of these two interacting states. In addition, 350 relative line intensities were measured from which the rotational expansions of the transition moment operators for the ν_1 and ν_3 states have been deduced. Finally, a complete listing of line positions, intensities, and lower state energies of the ν_1 and ν_3 bands of $^{16}O_3$ has been generated.

INTRODUCTION

Because of the importance of the ozone molecule in the earth's atmosphere, the vibration-rotation spectrum of this molecule has been the subject of numerous studies. The most recent investigations include the microwave works of Refs. (1-4), the study of the far-infrared spectrum (5), and the high resolution infrared studies of the regions of the ν_2 band (6-8), the ν_1 and ν_3 bands (4, 9-12), the $\nu_1 + \nu_3$ band (13), the $2\nu_3$, $\nu_1 + \nu_3$ and $2\nu_1$ bands (14), and the $\nu_1 + \nu_2 + \nu_3$ band (15). To improve the existing line parameters for the 10 μm region, which is often used in remote sensing studies, we have recorded spectra at 0.005 cm^{-1} resolution covering this interval with the McMath Fourier transform spectrometer at the National Solar Observatory on Kitt Peak. We have reanalyzed the ν_1 and ν_3 bands of $^{16}O_3$ from these spectra, and present in this paper molecular parameters which can be used to calculate improved line positions and intensities for these two interacting bands.

EXPERIMENTAL DETAILS AND ANALYSIS

The absorption cell used in our experiments consisted of a 50 cm-long, 5.08 cm-diameter Pyrex tube with Teflon valves. Slightly wedged (5-10 mrad) potassium chloride windows were used in order to prevent channeling arising from multiple reflections. The sample pressures ranged from 0.37 to 23.2 Torr of which three scans, listed in Table I, were selected for the

analysis. During the experiment, the pressures and temperatures were monitored continuously using 0 to 10 Torr and 0 to 100 Torr Barocel pressure heads and either a thermocouple or a mercury-in-glass thermometer placed in contact with the absorption cell. The ν_1 band lines of $^{14}N_2{}^{16}O$ between 1255 and 1282 cm^{-1}, as reported by Olson et al. (16), were used to calibrate the wavelength scale of the spectra.

The ozone samples were prepared using nearly pure (>99.98%) $^{16}O_2$ or natural O_2 samples. The standard technique of silent electric discharge was used in generating the ozone. For additional experimental details see Flaud et al. (17) and Rinsland et al. (18).

Using the results of previous studies of the ν_1 and ν_3 bands of $^{16}O_3$ (4, 9-11), it was rather easy to start the analysis of the spectra. Following the initial assignments, a first calculation was performed using a Hamiltonian, taking explicitly into account the Coriolis interaction between the rotational levels of the two interacting vibrational states (100) and (001) (see Table II). A first set of vibrational energies, rotational and coupling constants, was then obtained allowing us to calculate extrapolated levels and to extend the assignments. The process was repeated until almost all of the lines expected to be observable in the laboratory data were assigned. The interfering lines belonging to the hot bands were identified using the results of Ref. (10) whereas lines belonging to the ν_1 and ν_3 bands of the isotopic species $^{16}O^{18}O^{16}O$ and $^{16}O^{16}O^{18}O$ were located in the natural O_3 spectra with the aid of the results

given in Refs. (17-19). The 10 μm spectral region of O_3 is very crowded, even at the high resolution reached by the McMath Fourier transform spectrometer, and, in order to derive the most accurate energy levels, great care was taken to select only well isolated and unblended transitions for the analysis. In this respect, the availability of spectra recorded over a range of ozone pressures proved to be very useful. Finally, about 2600 lines belonging to the ν_1 and ν_3 bands of $^{16}O_3$ were used to derive the experimental upper state rotational energy levels (up to $J = 69$ and $K_a = 20$).

LINE POSITIONS

In order to derive precise rotational levels for the (100) and (001) vibrational states, we decided first to fit simultaneously the microwave (1-4) and far infrared (5) data to obtain a unique set of rotational constants for the ground state. This was done using a Watson-type Hamiltonian (Table II), and the values are given in Table III. The statistical weights used in this calculation were those given in Refs. (4, 5), and the observed line positions were reproduced within their stated experimental uncertainties. Then adding the observed wavenumbers of the ν_1 and ν_3 lines to the rotational energy levels of the ground state computed with the constants of Table III, we deduced the energies of the rotational levels of the (100) and (001) vibrational states. These last levels together with the available microwave data for these states (4) were least-squares

fitted using again the Hamiltonian matrix given in Table II. The results are very satisfactory since the infrared and microwave data are reproduced within their experimental uncertainties (standard deviations of 0.33×10^{-3} cm^{-1} for the infrared data and 0.11 MHz for the microwave data). The corresponding vibrational energies, rotational and coupling constants are given in Table IV. As noticed in previous works (4, 20), it was not possible to determine simultaneously all the coupling constants, and consequently $h'_{001,100}$, the coefficient of the operator iJ_y, was given a fixed value. This value has been derived from the potential function given in Ref. (21) and is compatible with the values of the same constant obtained for $^{16}O^{18}O^{16}O$ (17) and $^{18}O^{16}O^{18}O$ (22).

LINE INTENSITIES

The intensities of 350 lines belonging to the ν_1 and ν_3 bands of $^{16}O_3$ were measured from three spectra, the characteristics of which are given in Table I. However, since the exact amount of ozone was not known for each spectrum, we have used lines measured in the different spectra to calibrate each spectrum against the other in order to obtain a consistent set of relative intensities. These relative intensities were then reproduced using the method extensively described in Refs. (23, 24). The transformed transition moment operators of the ν_1 and ν_3 bands are expanded in the following way:

B-type band

$$(000)\ (100)\mu_z' = (000)\ (100)\mu_1'\ \phi_x + (000)\ (100)\mu_4'\ \{i\phi_y,\ J_z\} + (000)\ (100)\mu_5'\ \{\phi_z,\ iJ_y\} + \ldots$$

A-type band

$$(000)\ (100)\mu_z' = (000)\ (001)\mu_1'\ \phi_z + (000)\ (001)\mu_4'\ \frac{1}{2}\left(\{\phi_x,\ iJ_y\} - \{i\phi_y,\ J_x\}\right) + (000)\ (001)\mu_6'\ \frac{1}{2}\left(\{\phi_x,\ iJ_y\} + \{i\phi_y,\ J_x\}\right) + \ldots$$

with $\{A,\ B\} = AB + BA$

$\phi_\alpha = \Phi_{z\alpha}$ (direction cosine)

J_α = component of J along the molecular axis α.

Together with the wavefunctions derived from the diagonalization of the Hamiltonian matrices of the upper states and the ground state, the previous expansions were used to reproduce the observed line intensities leading to the determination of the transition moment constants $^{vv'}\mu_j'$ given in Table V. We have also quoted in this table the theoretical values of these constants derived using the formulae of Ref. (24) and the ozone dipole moment expansion given in Ref. (17). It is interesting to note that:

1) The correcting rotational constants appearing in the expansion of the transformed transition moment operator of the ν_3 band were fixed to their theoretical values. In fact, it was not possible to determine these values from our experimental set of intensities because their contribution is weak for the lines which were measured.

2) There is excellent agreement between the experimental and theoretical values of (000) (100)μ_4'. As already noticed in Ref. (4), this term is essential to reproduce correctly the ν_1 line intensities. The agreement is less satisfactory for the other correcting term, but this is explainable because the contribution of this last term is weaker, and consequently it is not well determined from our limited set of intensities.

Overall, the fit is very satisfactory since 82.3% of the intensities are reproduced within a relative error less than 12% (see the statistical analysis of Table V for more details).

As mentioned previously, it has not been possible to measure absolute intensities from our laboratory spectra. Many measurements of integrated band intensities (25, 26) or of individual line intensities (27, 28) of ozone have been performed in the 10 μm region, but the consistency in the results is not better than about 10%. Consequently, we have decided to scale our intensities using the value given in Refs. (4, 17, 28):

$$(\partial \mu_z / \partial q_3)_e = -0.2662 \text{ D}.$$

Finally, a complete spectrum of the ν_1 and ν_3 bands of $^{16}O_3$ has been computed[1] with an intensity cutoff of 0.1×10^{-24} cm^{-1}/molecule cm^{-2} at 296 K. In this computation maximum values of 89 and 23 were considered for J and K_a as well as a maximum lower state energy of 3500 cm^{-1}. Total band intensities of 0.5417×10^{-18} and 0.1413×10^{-16} cm^{-1}/molecule cm^{-2} at 296 K were obtained respectively for the ν_1 and ν_3 bands of $^{16}O_3$. The total band intensity obtained for ν_3 compares very well with the value of 0.1475×10^{-16} cm^{-1}/molecule cm^{-2} at 300 K derived by Secroun et al. (26) from the anomalous dispersion of ozone at 10 μm.

A listing of 14026 line positions, intensities, and lower state energies was derived, and to check its quality we have compared portions of synthetic spectra with the measured laboratory spectra. As can be seen from Figs. 1 and 2, the agreement between observation and calculation is very good. However, for atmospheric calculations, it should be recalled that the absolute intensities calculated in this work (as well as those for the ν_1 and ν_3 bands of $^{16}O^{18}O^{16}O$ (17) and $^{16}O^{16}O^{18}O$ (24)) have been obtained using $(\partial\mu_z/\partial q_3)_e = -0.2662$ D. If this value is to be changed, all of the intensities will have to be multiplied by the square of the ratio of the two values.

ACKNOWLEDGEMENTS

The authors thank Burnie Williams of NASA Langley and Rob Hubbard and Mike Brown of the National Solar Observatory (NSO)

for their help with with the laboratory experiment; Greg Ladd of NSO for the computer processing of the data; and D. Chris Benner of William and Mary and Carolyn H. Sutton of SASC Technologies for their assistance in the processing of the spectra at NASA Langley. Research at the College of William and Mary was supported under Cooperative Agreement NCC1-80 with NASA. J.-M. Flaud and C. Camy-Peyret acknowledge partial support of their research work under this cooperative agreement. The National Solar Observatory is operated by the Association of Universities for Research in Astronomy, Inc., under contract with the National Science Foundation. The computational work was performed at the Centre Inter Régional de Calcul Electronique, CNRS, 91405 Orsay, France.

---

[1] A partition function Z(296) = 3473 has been used in the intensity calculations.

REFERENCES

1. T. Tanaka and Y. Morino, J. Chem. Phys. 49, 2877-2878 (1968).

2. M. Lichtenstein, J.J. Gallagher, and S.A. Clough, J. Mol. Spectrosc. 40, 10-26 (1971).

3. J.C. Depannemaecker, B. Duterage, and J. Bellet, J. Quant. Spectrosc. Radiat. Transfer. 17, 519-530 (1977).

4. H.M. Pickett, E.A. Cohen, and J.S. Margolis, J. Mol. Spectrosc. 110, 186-214 (1985).

5. M. Carlotti, G. Di Lonardo, L. Fusina, A. Trombetti, A. Bonetti, B. Carli, and F. Mencaraglia, J. Mol. Spectrosc. 107, 89-93 (1984).

6. N. Monnanteuil, J.C. Depannemaecker, J. Bellet, A. Barbe, C. Secroun, P. Jouve, S. Giorgianni, Yan-Shek-Ho, and K. Narahari Rao, J. Mol. Spectrosc. 71, 399-413 (1978).

7. V. Malathy Devi, S.P. Reddy, K. Narahari Rao, J.-M. Flaud, and C. Camy-Peyret, J. Mol. Spectrosc. 77, 156-159 (1979).

8. A. Goldman, J.R. Gillis, D.G. Murcray, A. Barbe, and C. Secroun, J. Mol. Spectrosc. 96, 279-287 (1982).

9. A. Barbe, C. Secroun, P. Jouve, N. Monnanteuil, J.C. Depannemaecker, B. Duterage, J. Bellet, and P. Pinson, J. Mol. Spectrosc. 64, 343-364 (1977).

10. J.-M. Flaud, C. Camy-Peyret, and L.S. Rothman, Appl. Opt. 19, 655 (1980).

11. A. Barbe, C. Secroun, A. Goldman, and D.G. Murcray, J. Mol. Spectrosc. 86, 286-297 (1981).

12. M. El-Sherbiny, E.A. Ballik, J. Shewchun, B.K. Garside, and J. Reid, Appl. Opt. 18, 1198-1203 (1979).

13. A. Barbe, C. Secroun, P. Jouve, C. Camy-Peyret, and J.-M.Flaud,J. Mol. Spectrosc. 75, 103-110 (1977).

14. J.-M.Flaud, C.Camy-Peyret, A.Barbe, C.Secroun, and P. Jouve, J. Mol. Spectrosc. 80, 185-199 (1980).

15. A. Barbe, C. Secroun, A. Goldman, and J.R. Gillis, J. Mol. Spectrosc. 100, 377-381 (1983).

16. W.B. Olson, A.G. Maki, and W.J. Lafferty, J. Phys. Chem. Ref. Data 10, 1065-1084 (1981).

17. J.-M. Flaud, C. Camy-Peyret, V. Malathy Devi, C.P. Rinsland, and M.A.H. Smith, J. Mol. Spectrosc. 118, 334-344 (1986).

18. C.P. Rinsland, V. Malathy Devi, J.-M. Flaud, C. Camy-Peyret, M.A.H. Smith, and G.M. Stokes, J. Geophys. Res. 90, 10719-10725 (1985).

19. C. Camy-Peyret, J.-M. Flaud, A. Perrin, V. Malathy Devi, C.P. Rinsland, and M.A.H. Smith, J. Mol. Spectrosc. 118, 345-354 (1986).

20. V.I. Perevalov and V.G. Tyuterev, J. Mol. Spectrosc. 96, 56-76 (1982).

21. C. Camy-Peyret and J.-M. Flaud, Paper D11, Conference on Microwave Spectroscopy and Coherent Radiation, Durham, North Carolina (1979).

22. J.-M. Flaud, C. Camy-Peyret, V. Malthy Devi, C.P. Rinsland, and M.A.H. Smith, J. Mol. Spectrosc. (accepted for publication (1986).

23. J.-M. Flaud, C. Camy-Peyret, and R.A. Toth, "Water vapor line parameters from microwave to medium infrared". Pergamon Press, Oxford (1981).

24. C. Camy-Peyret and J.-M. Flaud, "Molecular Spectroscopy : Modern Research, vol.3", ed. K. Narahari Rao. Ch.2, Academic Press, Orlando (1985).

25. D.J. McCaa and J.H. Shaw, J. Mol. Spectrosc. 25, 374-397 (1968).

26. C. Secroun, A. Barbe, P. Jouve, Ph. Arcas, and E. Arié, J. Mol. Spectrosc. 85, 8-15 (1981).

27. C. Young and R.H.L. Bunner, Appl. Opt. 13, 1438-1443 (1974).

28. J.M. Hoell, Jr., C.N. Harward, C.H. Bair, and B.S. Williams, Opt. Eng. 21, 548-552 (1982).

TABLE I

Characteristics of the Spectra

Spectrum No	Pressure (Torr)	Temperature (K)	Path Length (cm)
1	23.2	293.1	50.0
2	8.1	295.7	50.0
3	1.09	293.1	50.0

TABLE II

Hamiltonian matrices

v = (100)	v'= (001)	
Watson-type Hamiltonian	Hermitic conj.	v = (000)
$H_{v\,v}$		Watson-type Hamiltonian $H_{v\,v}$
Coriolis interaction $H^{c}_{v',v}$	Watson-type Hamiltonian $H_{v',v'}$	

$$H_{v\,v} = E_v$$

$$+\left[A^v - \frac{1}{2}\left(B^v + C^v\right)\right] J_z^2 + \frac{1}{2}\left(B^v + C^v\right) J^2 + \frac{1}{2}\left(B^v - C^v\right) J_{xy}^2$$

$$-\Delta_K^v J_z^4 - \Delta_{JK}^v J_z^2 J^2 - \Delta_J^v (J^2)^2 - \delta_K^v \left\{J_z^2, J_{xy}^2\right\} - 2\delta_J^v J_{xy}^2 J^2$$

$$+H_K^v J_z^6 + H_{KJ}^v J_z^4 J^2 + H_{JK}^v J_z^2 (J^2)^2 + H_J^v (J^2)^3$$

$$+h_K^v \left\{J_z^4, J_{xy}^2\right\} + h_{KJ}^v \left\{J_z^2, J_{xy}^2\right\} J^2 + 2h_J^v J_{xy}^2 (J^2)^2$$

$$+L_K^v J_z^8 + L_{KKJ}^v J_z^6 J^2 + L_{KJ}^v J_z^4 (J^2)^2 + L_{KJJ}^v J^2 (J^2)^3 + L_J^v (J^2)^4$$

$$+l_K^v \left\{J_z^6, J_{xy}^2\right\} + l_{KJ}^v \left\{J_z^4, J_{xy}^2\right\} J^2 + l_{JK}^v \left\{J_z^2, J_{xy}^2\right\} (J^2)^2 + 2l_J^v J_{xy}^2 (J^2)^3$$

$$+P_K^v J_z^{10} + P_{KKKJ}^v J_z^8 J^2 + P_{KKJ}^v J_z^6 (J^2)^2 + \ldots$$

$$+p_K^v \left\{J_z^8, J_{xy}^2\right\} + p_{KKJ}^v \left\{J_z^6, J_{xy}^2\right\} J^2 + \ldots$$

$$H^c_{v',v} = h^c_{v',v} \{J_x, J_y\} + h^{c}_{v',v} i J_y + h^{c}_{v',v} \left\{J_z^2, \{J_x, J_z\}\right\}$$

$$+h^{\cdots c}_{v',v} \{J_x, J_z\} J^2 + h^{\cdots c}_{v',v} \left(J_-^3 - J_+^3\right)$$

TABLE III

Rotational constants of the ground state of $^{16}O^{16}O^{16}O$

A^v	3.553666502_3	$\pm$ 0.00000023
B^v	0.445283207_0	$\pm$ 0.000000030
C^v	0.394751807_6	$\pm$ 0.000000027
Δ_K^v	$(0.2116872_7$	$\pm$ 0.0000069) x 10^{-3}
Δ_{JK}^v	$(-0.184846_9$	$\pm$ 0.00006) x 10^{-5}
Δ_J^v	$(0.454169_1$	$\pm$ 0.000035) x 10^{-6}
δ_K^v	$(0.323240_4$	$\pm$ 0.000040) x 10^{-5}
δ_J^v	$(0.697903_5$	$\pm$ 0.000022) x 10^{-7}
H_K^v	$(0.39896_2$	$\pm$ 0.00087) x 10^{-7}
H_{KJ}^v	$(-0.18592_9$	$\pm$ 0.00047) x 10^{-8}
H_{JK}^v	$(-0.646_8$	$\pm$ 0.037) x 10^{-11}
H_J^v	$(0.321_5$	$\pm$ 0.013) x 10^{-12}
h_K^v	$(0.2293_3$	$\pm$ 0.0033) x 10^{-8}
h_{KJ}^v	$(-0.757_6$	$\pm$ 0.049) x 10^{-11}
h_J^v	$(0.1755_0$	$\pm$ 0.0011) x 10^{-12}
L_K^v	$(-0.1177_0$	$\pm$ 0.0031) x 10^{-10}
L_{KKJ}^v	$(0.273_9$	$\pm$ 0.043) x 10^{-12}
L_{KJJ}^v	$(-0.325_1$	$\pm$ 0.037) x 10^{-15}
L_J^v	$(0.299_4$	$\pm$ 0.071) x 10^{-17}
l_K^v	$(0.181_2$	$\pm$ 0.056) x 10^{-12}
P_K^v	$(0.333_0$	$\pm$ 0.033) x 10^{-14}
P_{KKKJ}^v	$(0.189_5$	$\pm$ 0.093) x 10^{-15}

All the results are given in cm^{-1}. The errors correspond to one standard deviation.

TABLE IV

Vibrational energies, rotational and coupling constants for the (100) and (001) vibrational states of $^{16}O_3$

E_v	1103.13728_5	$\pm$ 0.000023	1042.08398_4	$\pm$ 0.000023
A^v	3.55669374_9	$\pm$ 0.00000054	3.50055300_6	$\pm$ 0.00000052
B^v	0.442736468_2	$\pm$ 0.000000069	0.441296035_7	$\pm$ 0.000000053
C^v	0.392568221_0	$\pm$ 0.000000063	0.390998275_0	$\pm$ 0.000000048
Δ_K^v	$(0.217494_{60}$	$\pm$ 0.000010) $\times 10^{-3}$	$(0.208072_{36}$	$\pm$ 0.000012) $\times 10^{-3}$
Δ_{KJ}^v	$(-0.21569_{16}$	$\pm$ 0.00012) $\times 10^{-5}$	$(-0.16976_{94}$	$\pm$ 0.00012) $\times 10^{-5}$
Δ_J^v	$(0.461480_{61}$	$\pm$ 0.000053) $\times 10^{-6}$	$(0.456697_{12}$	$\pm$ 0.000034) $\times 10^{-6}$
δ_K^v	$(0.35570_{01}$	$\pm$ 0.00019) $\times 10^{-5}$	$(0.29609_{13}$	$\pm$ 0.00020) $\times 10^{-5}$
δ_J^v	$(0.658775_{18}$	$\pm$ 0.000098) $\times 10^{-7}$	$(0.759512_{71}$	$\pm$ 0.000064) $\times 10^{-7}$
H_K^v	$(0.41896_{90}$	$\pm$ 0.00058) $\times 10^{-7}$	$(0.39035_{67}$	$\pm$ 0.00080) $\times 10^{-7}$
H_{KJ}^v	$(-0.2040_{93}$	$\pm$ 0.0011) $\times 10^{-8}$	$(-0.1802_{30}$	$\pm$ 0.0012) $\times 10^{-8}$
H_{JK}^v	$(-0.312_{21}$	$\pm$ 0.014) $\times 10^{-10}$	$(0.15_{94}$	$\pm$ 0.15) $\times 10^{-11}$
H_J^v	$(0.423_{63}$	$\pm$ 0.013) $\times 10^{-12}$	$(0.1704_{04}$	$\pm$ 0.0070) $\times 10^{-12}$
h_K^v	$(0.97_{85}$	$\pm$ 0.12) $\times 10^{-9}$	$(0.248_{24}$	$\pm$ 0.013) $\times 10^{-8}$
h_{KJ}^v	$(-0.79_{98}$	$\pm$ 0.13) $\times 10^{-11}$	$(-0.1141_{99}$	$\pm$ 0.0074) $\times 10^{-10}$
h_J^v	$(0.916_{43}$	$\pm$ 0.038) $\times 10^{-13}$	$(0.2355_{10}$	$\pm$ 0.0021) $\times 10^{-12}$
L_K^v	$(-0.12188_{73}$	$\pm$ 0.00089) $\times 10^{-10}$	$(-0.1141_{28}$	$\pm$ 0.0015) $\times 10^{-10}$
L_{KKJ}^v	$(0.308_{39}$	$\pm$ 0.025) $\times 10^{-12}$	$(0.317_{37}$	$\pm$ 0.032) $\times 10^{-12}$
L_{KJJ}^v	-0.3251	$\times 10^{-15}$	-0.3251	$\times 10^{-15}$
L_J^v	0.2994	$\times 10^{-17}$	0.2994	$\times 10^{-17}$
J_K^v	$(0.14_{53}$	$\pm$ 0.13) $\times 10^{-12}$	$(0.21_{07}$	$\pm$ 0.17) $\times 10^{-12}$
P_K^v	0.333	$\times 10^{-14}$	0.333	$\times 10^{-14}$
P_{KKJ}^v	0.1895	$\times 10^{-18}$	0.1895	$\times 10^{-18}$

Coupling constants

$$h^{c}_{001.100} = (-0.996301_{67} \pm 0.000080) \times 10^{-2}$$
$$h'^{c}_{001.100} = -0.470$$
$$h''^{c}_{001.100} = (0.7568_{80} \pm 0.0031) \times 10^{-6}$$
$$h'''^{c}_{001.100} = (-0.10585_{06} \pm 0.00039) \times 10^{-6}$$
$$h''''^{c}_{001.100} = (0.58_{42} \pm 0.24) \times 10^{9}$$

All the results are given in cm^{-1} and the quoted errors correspond to one standard deviation. Parameters with no errors were held fixed.

TABLE V

Transition moment constants of the ν_1 and ν_3 bands of $^{16}O_3$

$^{vv'}\mu_j'$		Experimental	Theoretical
ν_3 band	μ_1'	-0.188232	-0.188232
	μ_4'	0.318×10^{-4}	0.318×10^{-4}
	μ_6'	0.853×10^{-5}	0.853×10^{-5}
ν_1 band	μ_1'	$(-0.15450_9 \pm 0.00061) \times 10^{-1}$	-0.154×10^{-1}
	μ_4'	$(-0.1802_4 \pm 0.0052) \times 10^{-3}$	-0.48×10^{-3}
	μ_5'	$(0.190_4 \pm 0.033) \times 10^{-4}$	0.549×10^{-5}

All the results are in Debye (D) and the quoted errors correspond to one standard deviation. For the constants without errors, the theoretical values have been used in the line intensity calculation (see text).

Statistical analysis

$$\delta = \frac{|I_{obs} - I_{calc}|}{I_{obs}}$$

$0 \leqslant \delta < 6$ %	55.7 % of the lines
$6 \leqslant \delta < 12$ %	26.6 %
$12 \leqslant \delta < 24$ %	24.0 %
$24 \leqslant \delta < 34$ %	3.7 %

Figure 1. Comparison between a weakly apodized laboratory spectrum (solid line) recorded with ≈0.37 Torr of $^{16}O_3$ in a 50-cm absorption path and a calculated spectrum (plus symbols) generated with the line parameters described in the text. Residuals (observed minus calculated) are plotted on expanded vertical scale in the upper panel and are expressed as a percentage of the peak measured intensity in the interval. Some absorption by hot band transitions of $^{16}O_3$ occurs this interval and has been simulated with the line parameters from the 1982 AFGL compilation. The mixing ratio of O_3 in the laboratory sample has been adjusted in matching the measured and calculated spectra. There are simultaneously high K_a ν_3 lines and resonating high K_a ν_1 lines in this region.

Figure 2. Comparison of a weakly apodized laboratory spectrum (solid line) recorded with ≈23.2 Torr of natural O_3 in a 50-cm absorption path and a calculated spectrum (plus symbols) generated with the line parameters described in the text. The format is the same as in Fig. 1. There are very high K_a ν_1 lines in this region.

Figure 1

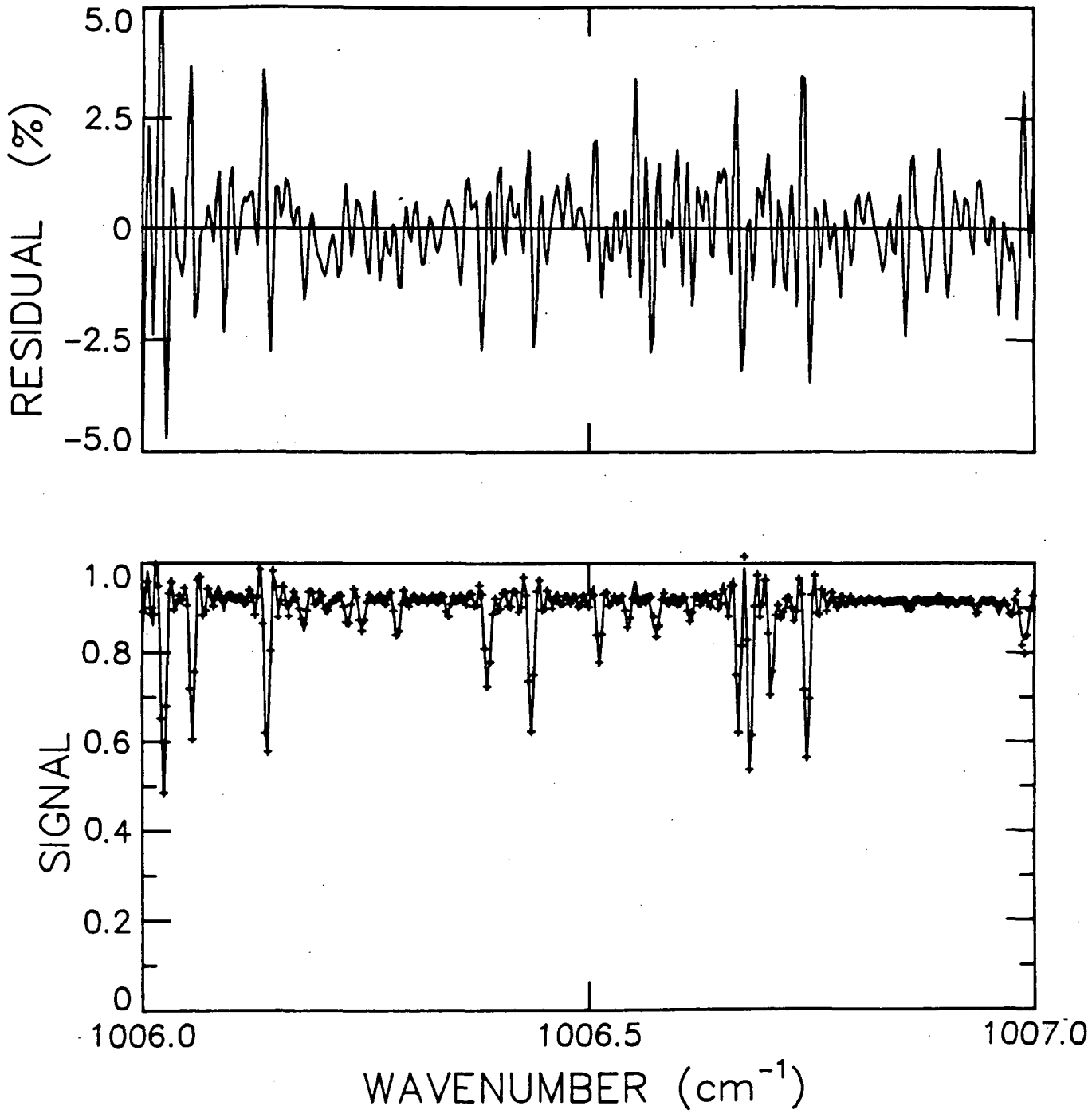
5.0
2.5
0
-2.5
-5.0
RESIDUAL (%)
1.0
0.8
0.6
0.4
0.2
0
SIGNAL
1006.0
1006.5
1007.0
WAVENUMBER (cm^{-1})

Figure 2

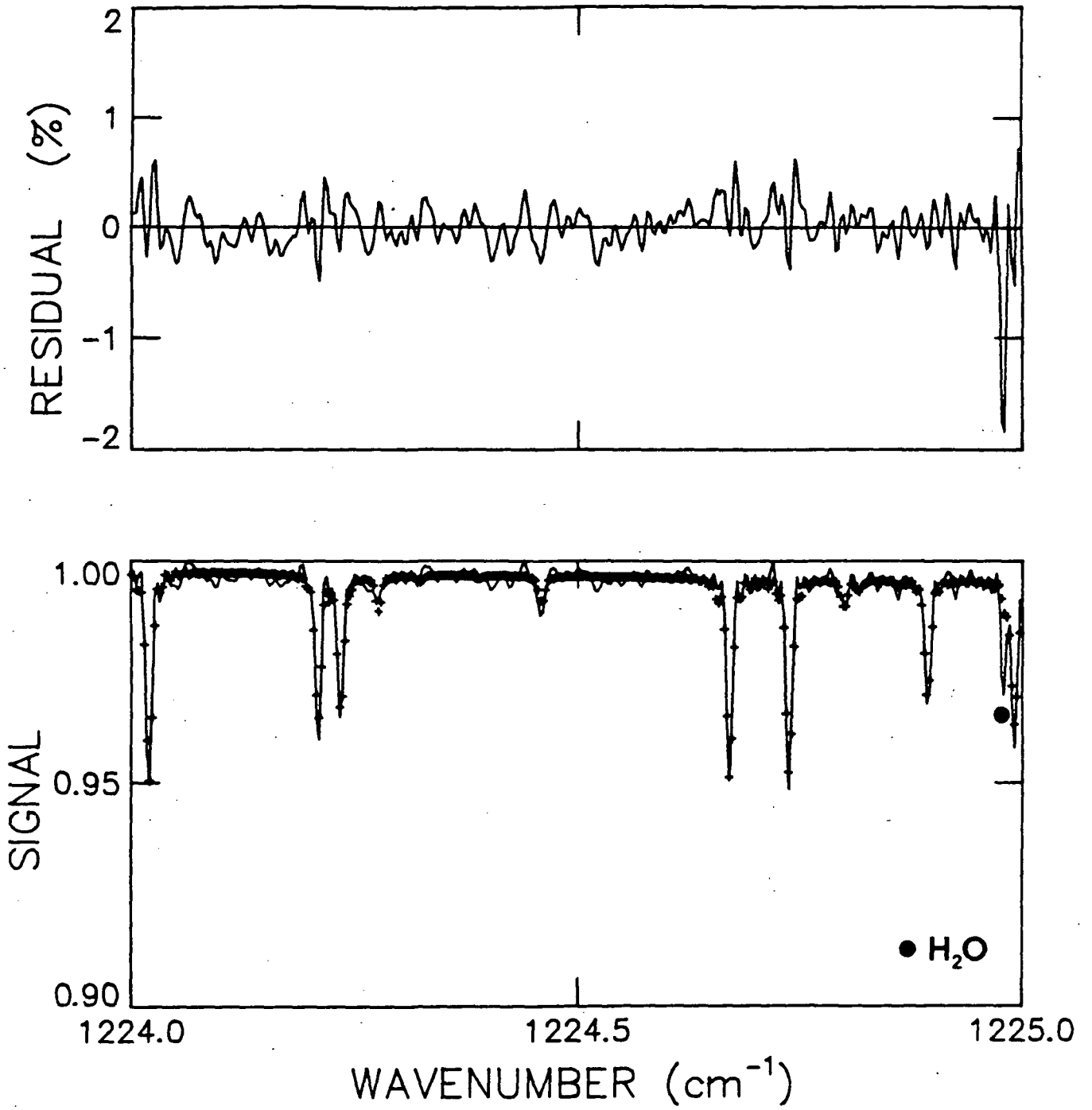
2
1
0
-1
-2
RESIDUAL (%)
1.00
0.95
0.90
SIGNAL
● H_2O
1224.0
1224.5
1225.0
WAVENUMBER (cm^{-1})

List of Symbols

ν - lower case Greek letter nu

γ - lower case Greek letter gamma

τ - lower case Greek letter tau

μ - lower case Greek letter mu

ϕ - lower case Greek letter phi

Δ - upper case Greek letter delta

δ - lower case Greek letter delta